Author's Accepted Manuscript

www.elsevier.com/locate/cageo

Representation of paleomagnetic data in virtual globes (a case study from the Pyrenees)

Tania Mochales, Thomas G. Blenkinsop

PII: S0098-3004(14)00140-X
DOI: http://dx.doi.org/10.1016/j.cageo.2014.05.013
Reference: CAGEO3388

To appear in: *Computers & Geosciences*

Received date: 25 November 2013
Revised date: 28 April 2014
Accepted date: 27 May 2014

Cite this article as: Tania Mochales, Thomas G. Blenkinsop, Representation of paleomagnetic data in virtual globes (a case study from the Pyrenees), *Computers & Geosciences*, http://dx.doi.org/10.1016/j.cageo.2014.05.013

Representation of paleomagnetic data in virtual globes (a case study from the Pyrenees)

Tania Mochales[a,b], Thomas G. Blenkinsop[c,d]

[a]Present Address: Istituto Nazionale di Geofísica e Vulcanologia, Via Arcivescovado 8, 67100 L'Aquila, Italy, taniamochales@gmail.com

[b]School of Earth Sciences, The University of Queensland, 4072 Brisbane, Australia

[c]School of Earth and Environmental Science, James Cook University, 4812 Townsville, Australia.

[d]Present Address: School of Earth and Ocean Science, Cardiff University, Main Building, Park Place, Cardiff CF10 3AT, United Kingdom, BlenkinsopT@Cardiff.ac.uk

Keywords: Virtual globe, KML, KMZ, Paleomagnetism, Google Earth, Visualization

Abstract

Virtual globes allow geo-referencing and visualisation of diverse geologic datasets. A vertical axis paleomagnetic rotation study in the Southern Pyrenees, Spain, is used to illustrate the potential of virtual globes for representing paleomagnetic data. A macro enabled workbook that we call P2K, allows KML files to be generated from conventional paleomagnetic datasets. Cones and arch models are used to represent the paleomagnetic vector, and the rotation with regard to the local reference direction, respectively. This visualization provides simultaneous representation of local magnetic declination, inclination and precise confidence cones, shown in their geographic position from diverse perspectives and scales.

1. Introduction

Past directions of the Earth's magnetic field are recorded in rocks, and following appropriate paleomagnetic analysis, they can be expressed as a vector (defined by intensity, declination and inclination) with confidence parameters (e.g. Van der Voo, 1990; Opdike and Channel, 1996). Classical representation of paleomagnetic vectors has been limited to 2D. Declination is thus expressed in maps (Figure 1), where authors may represent a local reference direction, and highlight ages or confidence angles, as in Figure 2 (e.g. Holt and Haines, 1993; Govers and Wortel 2005). In other cases, a map is shown with a qualitative palinspastic reconstruction (Figure 1a; e.g. Figure 9 in Speranza et al., 2002) and/or rotation arrows (Figure 1b, e.g. Figure 1 in Antolín et al, 2012 or Figure 1c, e.g. Figure 2 in Govers and Wortel, 2005); contoured plots of rotation angles (Figure 1d, e.g Figure 3 in Titus et al., 2011), or stereoplots of paleomagnetic poles can be also shown (Figure 1e e.g. Figure 6 in Soto et al., 2008). A considerable amount of work has been performed to compile paleomagnetic data in order to interpret tectonics, such as the Global Paleomagnetic database, (McElhinny and Lock, 1996) or MagIC (Tauxe et al., 2012). The Pyrenean Paleomagnetic Database (Lòpez et al., 2008; San Miguel et al., 2010; Pyrenean Pmag DB, IGME) is the first paloemagnetic dataset conceived at the orogen scale using geologic maps as the main background.

During the last few years virtual globes have been adopted in response to the needs of the scientific, pedagogic and industrial communities (e.g. SERC, Pedagogy in Action; World Wind, NASA). Virtual globes can geo-reference geologic datasets as diverse as maps and cross-sections (Google Earth profile, De Paor and Whitmeyer, 2011), world magnetic declination (Google Compass), coal exploitation (e.g. Queensland Coal

Mines, Queensland Government Department of Natural Resources, Mines and Water; Vizmap, Google Earth Applications), dams and freshwater lakes (e.g. SEQ Water, Geospatial Information and Technology Association [GITA]; Vizmap, Google Earth Applications), and geological mapping (SIGECO, Instituto Geológico y Minero de España) among others, which testify to the versatility and widespread use of this tool. Virtual globes have become very helpful in structural geology visualization (Simpson and De Paor, 2009; De Paor and Whitmeyer, 2011; Blenkinsop, 2012; Martínez-Torres et al., 2012) since they can display topography and geology, and allow quick shifts of user's viewpoint and scale. Based on this background, we intend that paleomagnetic data be included among the geological datasets that can be represented in Google Earth.

The open-source Keyhole Markup Language (KML) represents a great advance for virtual globes. KML is an XML-based language that manages the display of 3D geospatial data, which has become widespread in scientific research relying on virtual globes (De Paor et al., 2012). KML enables users to customize data in ways as varied as Shapefiles in ArcGIS. These capacities are possible in combination with COLLADA (COLLAborative Design Activity) models, generated, for example by SketchUp and other 3D modelling applications (De Paor and Whitmeyer, 2011). In this paper we used the free SketchUp (now SketchUp Make) application to create a symbology for representing paleomagnetic data in virtual globes.

We propose a protocol for the symbology that achieves a clear distinction between clockwise and anticlockwise paleomagnetic rotations (Figure 3), and normal and reverse polarity, as well as an indication of the confidence parameters. These data can be easily and well represented in a virtual globe, providing not only information about declination but also inclination (often omitted from 2D representations). A local reference direction can also be shown for any rotation. We provide a macro-enabled spreadsheet (P2K) that expresses the paleomagnetic data using the symbology via a KML file, allowing it to be presented and displayed in bird's eye views and through 360º viewpoints in virtual globes. Pop-ups with numerical and bibliographic information are included. This approach allows easy visualisation and compilation of paleomagnetic data, promoting the creation of geo-referred databases. We illustrate the method with a case study from the Pyrenees.

2. Case Study: The Boltaña Anticline

The Boltaña anticline, in the Southern Pyrenees, is a 25 km long, north-south oriented fold located westwards of the South Pyrenean central Unit (SPCU), which is a thrust-and-fold system transported south in piggyback sequence during Eocene times (Puigdefàbregas et al., 1975). Contemporary with the slow westwards propagation of south-transported thrust sheets, numerous structures transverse to the Pyrenean trend (WNW-ESE) were formed, such as the Boltaña anticline. The strata involved were coevally deposited through Eocene times, including a pre-folding stage of limestones in a platform sequence (56-49 Ma), overlain by slope rocks in an incipient synfolding setting in the Boltaña anticline (49-43 Ma). Next, deltaic progradation occurred through the eastern flank of the Boltaña anticline (43-41 Ma), followed by continental deposition (41-35 Ma) (Mochales et al., 2012a and references therein). Lutetian to Bartonian sediments (49-38 Ma) with growth-strata geometries record successive non-coaxial deformational episodes. Firstly, the folding of the Boltaña anticline took place ~43 Ma (Lutetian, Puigdefàbregas, 1975; Fernández et al., 2004; Mochales et al., 2010; Muñoz et al., 2013). Later, a clockwise rotation of the Boltaña thrust sheet, during 41-

35 Ma, explains the obliquity of the anticline with respect to the Pyrenean trend (Mochales et al., 2012b). Exposure is excellent, and the area has an acceptable Google Earth aerial image and DEM, making for a very suitable case study.

3. Representation of paleomagnetic data in virtual globes

Previous works that visualized structural geology data (e.g. Whitmeyer et al., 2010; Blenkinsop, 2012), opened new perspectives in virtual globe visualization and inspired the creation of paleomagnetic symbols in SketchUp (available freely from Trimble now as SketchUp Make) in this study, using COLLADA models like those created for representing structures.

Paleomagnetic data are usually organized in spreadsheets for final representation on digital maps, analysis and interpretation. Data should meet several reliability criteria such as laboratory, processing and statistical procedures as well as geological and geomagnetic constraints (Van der Voo, 1990; Fisher, 1953). They are then commonly compiled in rows where intensity of the magnetization and paleomagnetic vectors from the coordinate reference system (in situ) to the paleogeographical one (bedding correction) is shown (declination and inclination). Confidence angles (α95), and paleopoles corresponding to the age of the case study and author of the site are also documented.

The COLLADA models used to represent the paleomagnetic data (Figure 3) permit visualisation in virtual globes more intuitively than standard map symbols. The models were created in SketchUp, and are provided in supplementary information with this paper (Appendix A). The models consist of two cones, one to represent the paleomagnetic remanent vector, and one to show the confidence cone. The models are 3D representations of a common 2D paleomagnetic symbol. The cones are transparent so that they do not disturb the background, and encompass α95 from 1º to 60º, indicating the semi-angle of confidence from Fisher (1953) statistics. The models have long dimensions of 16 m, appropriate to an outcrop scale. These cones are duplicated to represent reverse or normal polarity with black or white versions respectively. The cones are shown elevated above the ground surface, and the base of the cone is connected to the ground at the observation site with a vertical line, allowing a clearer visualization of the background. The size of the cones and their height are adjustable in P2K according to the scope of the work.

The greatest advantage of this 3D representation compared to previous 2D methods is that the inclination component of the paelomagnetic vector of each site can be visualised, and with respect to the local reference direction. Classical 2D representations only allow visualization of the declination of the paleomagnetic vector, concealing the inclination component, which can be highly disturbed, especially when differential lithostatic loading produces inclination errors (Bilardello and Kodama, 2010). The greater ease of examining the inclination affords new insights into the degree of magnetic inclination perturbation throughout the rotational process. Quick assessment of inclination anomalies with regard to the paleopole characteristic of the geological time in question can be made (Figure 4). Another interesting advantage is the proper representation of the α95 confidence cone, which has a 3D attribute and is usually incorrectly projected in a 2D plane. A correction factor has to be introduced to the rotation error (Demarest, 1983) to represent the projection of a95 in a plane properly. Alternatively, the equation α95/cos (Inc) can accurately determine the 2D projection of α95 (Butler, 1992). Both calculations can be avoided by the correct representation of the error in 3D. This representation of paleomagnetic data in 3D is especially effective in combination with representation of structural data (e.g. S2K, Blenkinsop, 2012), which allows a first glance at the relationship between structural and paleomagnetic directions (Figure 5).

It is also useful to have a direct representation of vertical axis rotations with regard to the local reference direction. In P2K this is possible using an arch model, in which a curved arrow (arch) shows the rotation, distinguished by colour between clockwise and anticlockwise rotations. By means of the case study of the Boltaña anticline we can illustrate variations in the amount of vertical axis rotation (Figure 4). The younger sites, located towards the south, underscore the more striking rotation corresponding to the Priabonian age. Figure 4 shows the difference between the northwestern (older) sites, that underwent around 40º of rotation, compared to the southeastern sites (younger) that are closer to the Eocene reference (close to the current magnetic north) and therefore less rotated.

4. Data Input and KML file generation with P2K

The P2K spreadsheet can be downloaded from the Journal web site (Appendix A). It requires Excel in a macro-enabled version, and it is usable in any operating system that can run Excel. Two versions are offered: P2K.xlsm works with Excel 2011 for Macintosh and Windows, while P2K.xls works for Excel 2007 for Windows and Excel 2004 for Macintosh. The paleomagnetic input data are: Site name, Geographic coordinates, Rotation angle, Inclination, α95 confidence angle, Polarity, Author, Direction of paleomagnetic reference North, and inferred clockwise (C) or anticlockwise (A) direction of rotation. UTM coordinates are optional. Normal (N) and Reverse (R) polarities are accepted, as well as normalized polarity: antipodal Reverse polarity (-R). These normalized polarities are used when poles correspond to the antipodal direction of the majority of the dataset, making the normal and reverse directions commensurate.

The organisation of the P2K spreadsheet is as follows. In the first row, cell A2 contains a name that is used for folders within the KML document, which takes the name of the spreadsheet. Cell A4 contains a value for a scale, which multiplies the 16 m dimension of the cones symbol to an appropriate value if necessary. Cell A6 contains a height value that sets the height of the symbol above the ground level in metres. Data entry begins in row 3. The first column of cells corresponds to the site label. The next four columns correspond to the geographic coordinates (second and third in UTM, forth and fifth in decimal degrees). Coordinate information must be entered in WGS84 datum because that is the datum used by Google Earth. The sixth and seventh columns correspond to the Declination and Inclination angles. The α95 angle is located in the eighth column, polarity in the ninth and source author in the tenth. The reference declination and sense of rotation are entered in the final two columns. The paleomagnetic information can be read in a pop-up balloon.

The code necessary to represent the paleomagnetic information by generating a KLM file resides in the macro of the spreadsheet, which can be run from the Macro menu. The macro creates a KML file with three folders: the first is called *Symbol* and refers to the cones that represent the remanent paleomagnetic vectors. The second (*Data*) refers to the information that is displayed in the balloons, and the site names. The third

(*Rotation symbol*) refers to the arch symbol that indicates the vertical axis rotation. Each of the folders can be turned on and off independently in the Places panel of Google Earth.

The KML document calls on the *Symbols* and *arches* models that are kept in folders of ~~that name~~. The P2K spreadsheet and these folders must be placed in a single folder on the user's computer storage. The P2K folder supplied contains the P2K.xls and ~~P2Kxlms~~ spreadsheets, the Boltañaexample.kml example, and the symbols and arches folders. P2K ReadMe contains more detailed instructions about running the macro.

An alternative approach could be to enter data into a Fusion Table linked to a PHP, Python or Ruby script, which could output the Google Earth API embedded in a web page (De Paor et al., 2012). The macro code could also be adapted to generate the kml files with other applications that implement Visual Basic.

5. Conclusions

Virtual Globes are increasingly used by geologist to represent field data. They are a quick and economic way to store and share information. P2K is a macro-enabled Excel workbook to generate KLM files from paleomagnetic data, for visualization in virtual globes. Advantages of representing paleomagnetic data in the manner proposed here are visualisation of both declination and inclination simultaneously, accurate representation of confidence cones, and the ability to examine data sets in their geographic context with rapid change of scale and perspective.

Acknowledgements

TM acknowledges one-year postdoctoral fellowship from ARC-DP0986762 project (UQ) and current researcher contract from FIRB-ABRUZZO (INGV). We are also grateful to Juanjo Villalaín for his advice on this work. Mark Stokes put in a great effort to create the SketchUp models of the arches. Detailed comments from Emilio L. Pueyo and two other anonymous reviewers are appreciated.

Appendix A. Supporting Information

Supplementary data associated with this article – the P2K folder – can be found in the online version at

References

Antolín, B., Appel, E., Gloaguen, R., Dunkl, I., Ding, L., Montomoli, C., Liebke, U., Xu, Q., 2010, Paleomagnetic evidence for clockwise rotation and tilting in the eastern Tethyan Himalaya (SE Tibet): Implications for the Miocene tectonic evolution of the NE Himalaya. Tectonophysics 493, 172-186.

Bentham, P.A., 1992. The tectono-stratigraphic development of the western oblique ramp of the south-central Pyrenean thrust system, Northern Spain. Ph.D. thesis, University of Southern California. 253 p.

Blenkinsop T.G., 2012, Visualizing structural geology: From Excel to Google Earth, 52-56. In Computers & Geosciences, 45, 52-56.

Butler, R.F., 1992, Paleomagnetism, Magnetic Domains to Geologic Terranes, Boston, Blackwell, 319 p.

COLLADA, COLLAborative Design Activity. http://www.khronos.org/collada/ (accessed 6.3.14)

De Paor, D., Whitmeyer, S.J., 2011, Geological and geophysical modelling on virtual globes using KML, COLLADA, and Javascript. Computers and Geosciences 37, 100–110.

De Paor, D., Whitmeyer, S.J., Marks, M., Bailey, J.E., 2012, Geoscience applications of client/server scripts, Google Fusion Tables, and dynamic KML. Geological Society of America Special Papers, 492, p. 77-104. doi: 10.1130/2012.2492(06)

Demarest, H.H., 1983, Error analysis for the determination of tectonic rotation from paleomagnetic data. Journal of Geophysical Research, 88, B5, 4321-4328.

Fernández, O., Muñoz, J.A., Arbués, P., Falivene, O., Marzo, M., 2004, Three-dimensional reconstruction of geological surfaces: an example of growth strata and turbidite systems from the Ainsa Basin, Pyrenees, Spain. American Association of Petroleum Geologists Bulletin 88 (8), 1049-1068.

Fisher, R.A., 1953. Dispersion on a sphere. Proc. R. Soc. London Ser. A 217, 295-305.

Google Compass. http://googlecompass.com/ (accessed 22.4.14)

Google Earth Profile. http://library.usask.ca/murray/data-and-gis/GISpages/HowdoIfolder/HowdoIelevationinGoogleEarth.pdf (accessed 22.4.14)

Govers, R. and Wortel, M.J.R., 2005, Lithosphere tearing at STEP faults: Response to edges of subduction zones. Earth and Planetary Science Letters, 236, 505– 523.

Holt, W.E., and Haines, A.J., 1993, Velocity fields in deforming Asia from the inversion of earthquake-released strains: Tectonics, v. 12, p. 1–20.

Bilardello, D., Kodama, K.P., 2010, A new inclination shallowing correction of the Mauch Chunk Formation of Pennsylvania, based on high-field AIR results: Implications for the Carboniferous North American APW path and Pangea reconstructions, Earth Planet. Sci. Lettrs., 299, 218-227.

KML, World Wide Web Consortium. http://www.w3.org/(accessed 22.4.14)

Krijgsman, W., and Tauxe, L., 2004, Shallow bias in the Mediterranean palaeomagnetic directions caused by inclination error. Earth and Planetary Science Letters 222 (2), 685–695.

López, M.A., Oliván, C., Oliva, B., Pueyo, E.L. and the GeoKin3DPyr group, 2008. Pyrenean paleomagnetic databases. Geotemas, 10, 1219-1222.

Martínez-Torres, L.M., Lopetegui, A., Eguiluz, L., 2012, Automatic resolution of the three-points geological problem. Computers & Geosciences, 42, 200-202.

Mattei, M., Cifelli, F., D'Agostino, N., 2007, The evolution of the Calabrian Arc: Evidence from paleomagnetic and GPS observations. Earth and Planetary Science Letters 263, 259–274

McElhinny, M.W. and Lock, J., 1996, IAGA paleomagnetic databases with Access, Surv. Geophys.,17,575-591.

Mochales, T., Pueyo, E.L., Casas, A.M., Barnolas, A., Oliva-Urcia, B., 2010. Anisotropic magnetic susceptibility record of the kinematics of the Boltaña Anticline (Southern Pyrenees): Geological Journal, v. 45, p. 562-581, doi: 10.1002/gj.1207

Mochales, T., Barnolas, A., Pueyo, E.L., Serra-Kiel, J., Casas, A.M., Samsó, J.M., Ramajo, J., Sanjuán, J., 2012a, Chronostratigraphy of the Boltaña anticline and the Ainsa Basin (Southern Pyrenees). Geological Society of America Bulletin. doi:10.1130/B30418.1.

Mochales, T., Casas, A.M., Pueyo, E.L., Barnolas, A., 2012b, Rotational velocity for oblique structures (Boltaña anticline, Southern Pyrenees). Journal of Structural Geology 35 (2012) 2-16. doi:10.1016/j.jsg.2011.11.009.

Mümtaz Hisarlı, Z., 2011, New paleomagnetic constraints on the late Cretaceous and early Cenozoic tectonic history of the Eastern Pontides. Journal of Geodynamics, 52, Issue 2, 114–128.

Muñoz, J.A., Beamud, B., Fernández, O, Arbués, P., Dinarès-Turell, J., Poblet, J., 2013, The Ainsa fold and thrust oblique zone of the central Pyrenees: Kinematics of a curved contractional system from paleomagnetic and structural data. Tectonics 32 (59), 1142-1175.

Opdike, N.D, Channell, J.E.T., 1996, Magnetic Stratigraphy. International Geophysical Series, 64, Academic Press, San Diego. 346 pp.

Puigdefàbregas, C. ,1975, La sedimentación molásica en la cuenca de Jaca. Pirineos 104, 1–188.

Pyrenean Pmag DB. http://www.igme.es/infoigme/aplicaciones/paleomag (accessed 22.4.14)

Queensland Coal Mines, Queensland Government Department of Natural Resources, Mines and Water; Vizmap, Google Earth Applications. Vizmap, Google Earth Applications. http://www.vizmap.com.au/services/google-earth-applications/ (accessed 22.4.14)

San Miguel, G., Hernández, R., Pueyo, E.L. and the Geokin3DPyr, 2010, Pyrenean Paleomagnetic Database; Concept, state-of-the-art, and web interface design. Proceedings MAGIBER VI, 50-53.

SERC, Pedagogy in Action. http://serc.carleton.edu/sp/library/google_earth/how.html (accessed 22.4.14)

SEQ Water, Geospatial Information and Technology Association [GITA]; Vizmap, Google Earth Applications. Vizmap, Google Earth Applications. http://www.vizmap.com.au/services/google-earth-applications/ (accessed 22.4.14)

SIGECO, Instituto Geológico y Minero de España, Ministerio de Economía y Competitividad. http://cuarzo.igme.es/sigeco/Default.aspx (accessed 6.3.14)

Simpson, C., De Paor, D.G., 2009, Restoring maps and memoirs to four-dimensional space using virtual globe technology: a case study from the Scottish Highlands. In: Law, R.D., Butler, R.W.H., Holdsworth, R.E., Krabbendam, M., Strachan, R.A. (Eds.), Continental Tectonics and Mountain Building: The Legacy of Peach and Horne, 335. Geological Society of London Special Publication, pp. 427–439.

Speranza, F., Villa, I.M., Sagnotti, L., Florindo, F., Cosentino, D., Cipollari, P., Mattei, M., 2002, Age of the Corsica-Sardinia rotation and Liguro-Provencal Basin spreading: New paleomagnetic and Ar/Ar evidence. Tectonophysics 347: 231-251. doi:10.1016/S0040-1951(02)00031-8.

Soto, R., Villalaín J.J., Casas-Sainz, A.M,, 2008, Remagnetizations as a tool to analyze the tectonic history of inverted sedimentary basins: A case study from the Basque-Cantabrian basin (north Spain). Tectonics, Vol. 27, TC1017, doi:10.1029/2007TC002208, 2008

Taberner, C., Dinarés-Turell, J., Jiménez, J., Docherty, C., 1999, Basin infill architecture and evolution from magnetostratigraphic cross-basin correlations in the southeastern Pyrenean foreland basin: Geological Society of America Bulletin, 11(8), p. 1155-1174.

Tauxe, L., Constable, C.G., Jarboe, N., Koppers, A.A.P., Minnett, R., Shaar, R., 2012, PmagPy: Software package for paleomagnetic data analysis and gateway to the

Magnetics Information Consortium (MagIC) Database. Geochemistry, Geophysics, Geosystems doi: 10.1029/0000.

Titus, S.J., Crump, S., McGuire, Z., Horsman, E., Housen, B., 2011, Using vertical axis rotations to characterize off-fault deformation across the San Andreas Fault system, central California. Geology 39: 711-714.

Van der Voo, R., 1990, The reliability of paleomagnetic data. Tectonophysics 184, 1-9.

Vizmap, Google Earth Applications. http://www.vizmap.com.au/services/google-earth-applications/ (accessed 22.4.14)

Whitmeyer, S.J., Nicoletti, J., De Paor, D.G., 2010, The digital revolution in geologic mapping. GSA Today: A Publication of the Geological Society of America, vol. 20, doi:10.1130/GSATG70A.1.

World Wind, NASA. http://goworldwind.org/demos/(accessed 22.4.14)

Figure Captions

Figure 1. Ways of displaying paleomagnetic information in the literature. a) Paleomagnetic vectors shown with palinspastic reconstruction, modified ~~form~~ Speranza et al., (2002); b) Paleomagnetic vectors shown as vertical axis ~~rotation~~ with respect to the north, modified from Antolín et al., (2012); c) Rotation symbols show the regionally observed sense of motion on transform faults, or paleomagnetic rotations about a vertical axis, from Govers and Wortel, (2005). d) Paleomagnetic group means are superimposed over contoured rotation maps, from Titus et al., (2011). e) Equal area projections showing the site-mean paleomagnetic directions with their associated a95, from Soto et al., (2008).

Figure 2. Rotations in map view (arrows represent the magnetic declination and the confidence angle), modified from Mochales et al. (2012b).

Figure 3. Examples of models created in SketchUp. Rotation is the angle difference between the local declination and the local reference direction. Due to 3D representation, we can illustrate inclination and the α95 confidence angle correctly.

Figure 4. Boltaña anticline case study. Normal polarities (black arrows) plunge into the earth in the northern hemisphere and reverse polarities (white arrows) emerge from the earth. Here, reverse polarities have been normalized (-R) to be comparable with others and an Eocene reference (Taberner et al., 1999). A rotation can be appreciated in younger materials (Priabonian) towards the southeast, as well as inclination and confidence angle of each site. The figure illustrates the area where the rapid vertical axis rotation was detected from map view (a), oblique view (b) and horizontal view (c)

Figure 5. Oblique view of a northern area where paleomagnetic data (P2K) and structural data (SK2) are here combined to get a realistic understanding of the paleomagnetic and tectonic record.

Figure 1

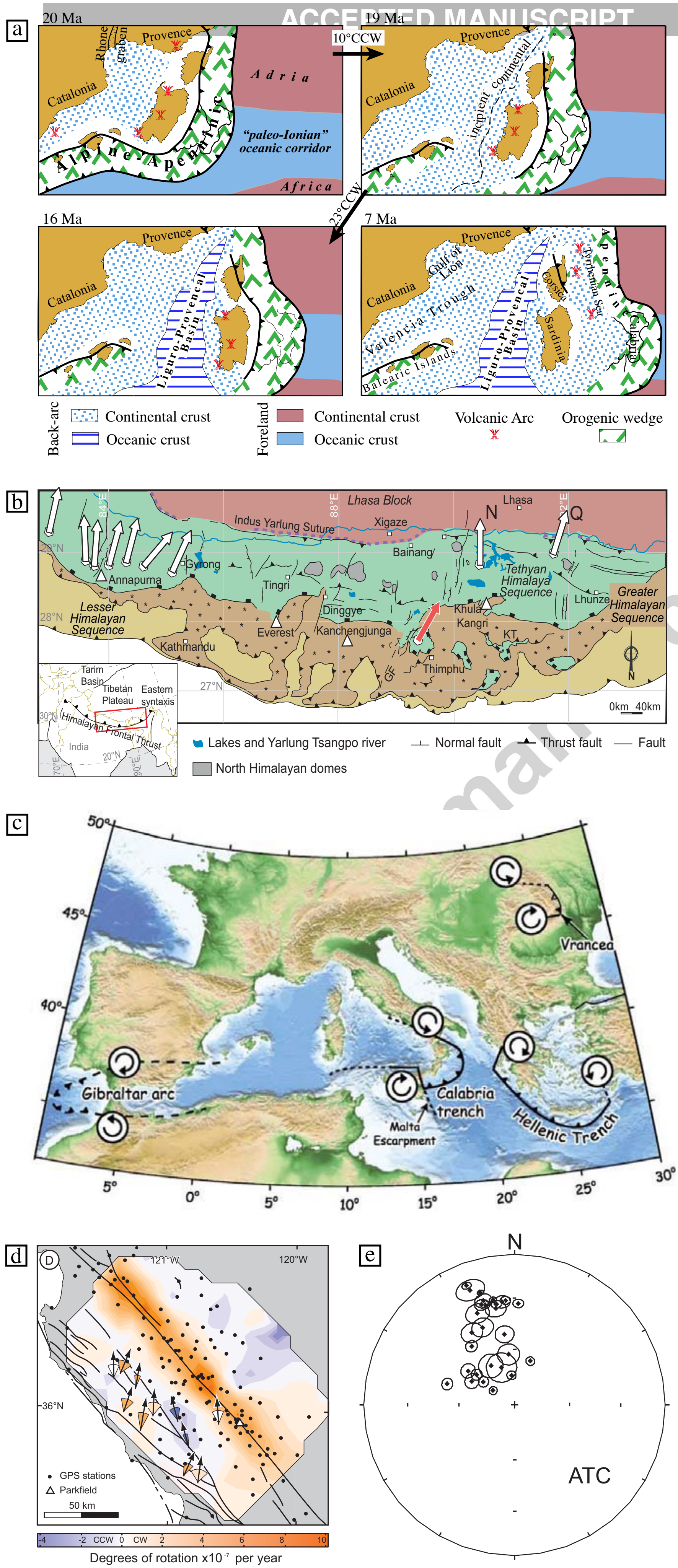
a
20 Ma
Rhone graben
Provence
Catalonia
Adria
"paleo-Ionian" oceanic corridor
Alpine-Apennine
Africa
19 Ma
10°CCW
incipient continental
23°CCW
16 Ma
Liguro-Provencal Basin
7 Ma
Gulf of Lion
Valencia Trough
Balearic Islands
Corsica
Sardinia
Tyrrhenian Sea
Apennine
Calabria
Back-arc
Continental crust
Oceanic crust
Foreland
Continental crust
Oceanic crust
Volcanic Arc
Orogenic wedge
b
Lhasa Block
Lhasa
Indus Yarlung Suture
Xigaze
Bainang
84°E
88°E
92°E
N
Q
29°N
28°N
27°N
Gyirong
Annapurna
Tingri
Dinggye
Everest
Kanchengjunga
Kathmandu
Lesser Himalayan Sequence
Tethyan Himalaya Sequence
Greater Himalayan Sequence
Khula Kangri
KT
Lhunze
Thimphu
GF
0km 40km
Tarim Basin
Tibetan Plateau
Eastern syntaxis
Himalayan Frontal Thrust
India
30°N
20°N
70°E
90°E
Lakes and Yarlung Tsangpo river
Normal fault
Thrust fault
Fault
North Himalayan domes
c
50°
45°
40°
Vrancea
Gibraltar arc
Calabria trench
Malta Escarpment
Hellenic Trench
5°
0°
5°
10°
15°
20°
25°
30°
d
D
121°W
120°W
36°N
GPS stations
Parkfield
50 km
-4
-2
CCW
0
CW
2
4
6
8
10
Degrees of rotation x10⁻⁷ per year
e
N
ATC

Figure 2

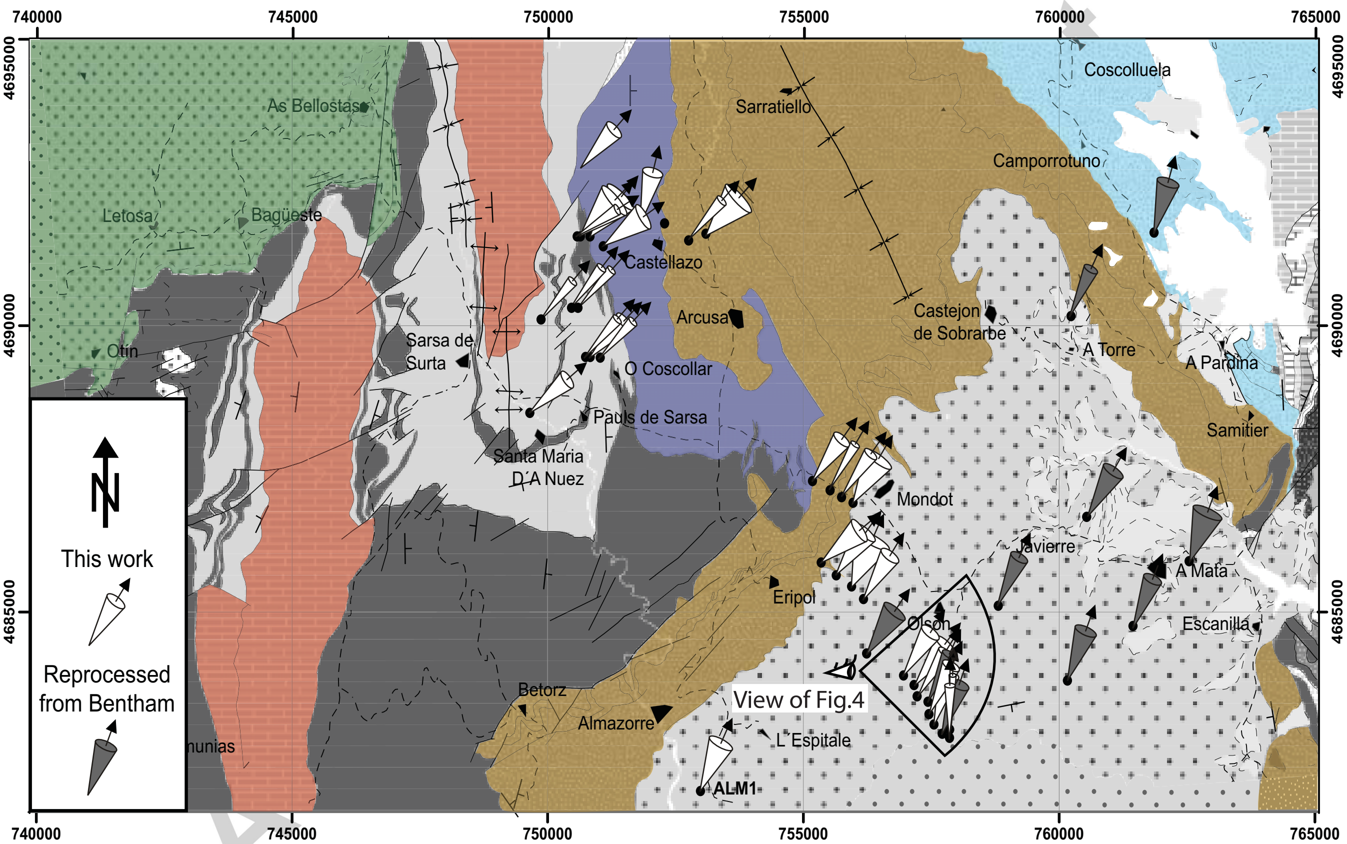
740000
745000
750000
755000
760000
765000
4695000
4690000
4685000
As Bellostas
Letosa
Bagüeste
Otin
Sarsa de
Surta
Sarratiello
Castellazo
Arcusa
O Coscollar
Pauls de Sarsa
Santa Maria
D´A Nuez
Coscolluela
Camporrotuno
Castejon
de Sobrarbe
A Torre
A Pardina
Samitier
Mondot
Javierre
A Mata
Eripol
Olson
Escanilla
Betorz
Almazorre
View of Fig.4
L´Espitale
ALM1
This work
Reprocessed
from Bentham

Figure 3

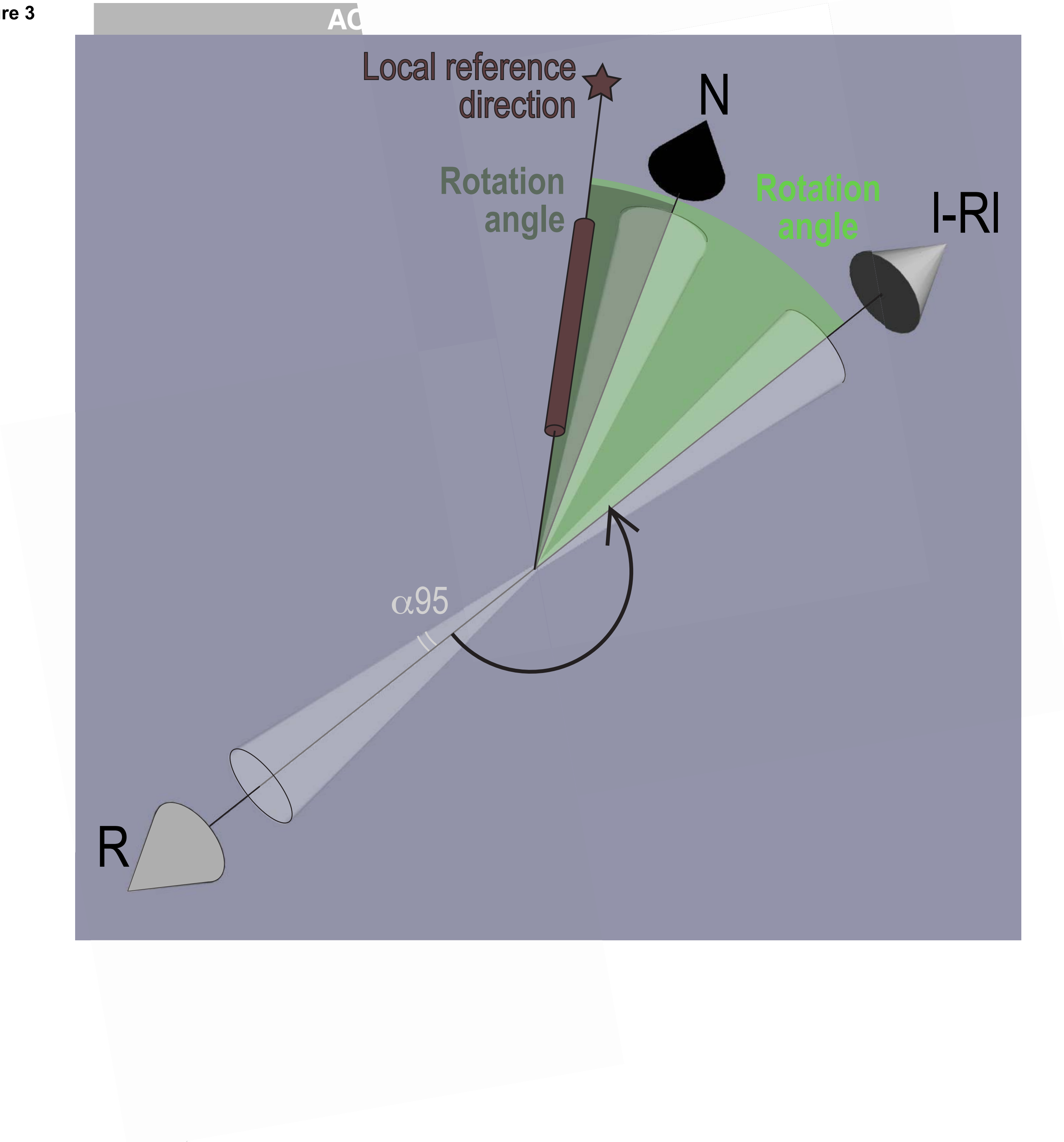

AC
Local reference direction
N
Rotation angle
Rotation angle
I-RI
α95
R

Figure 4

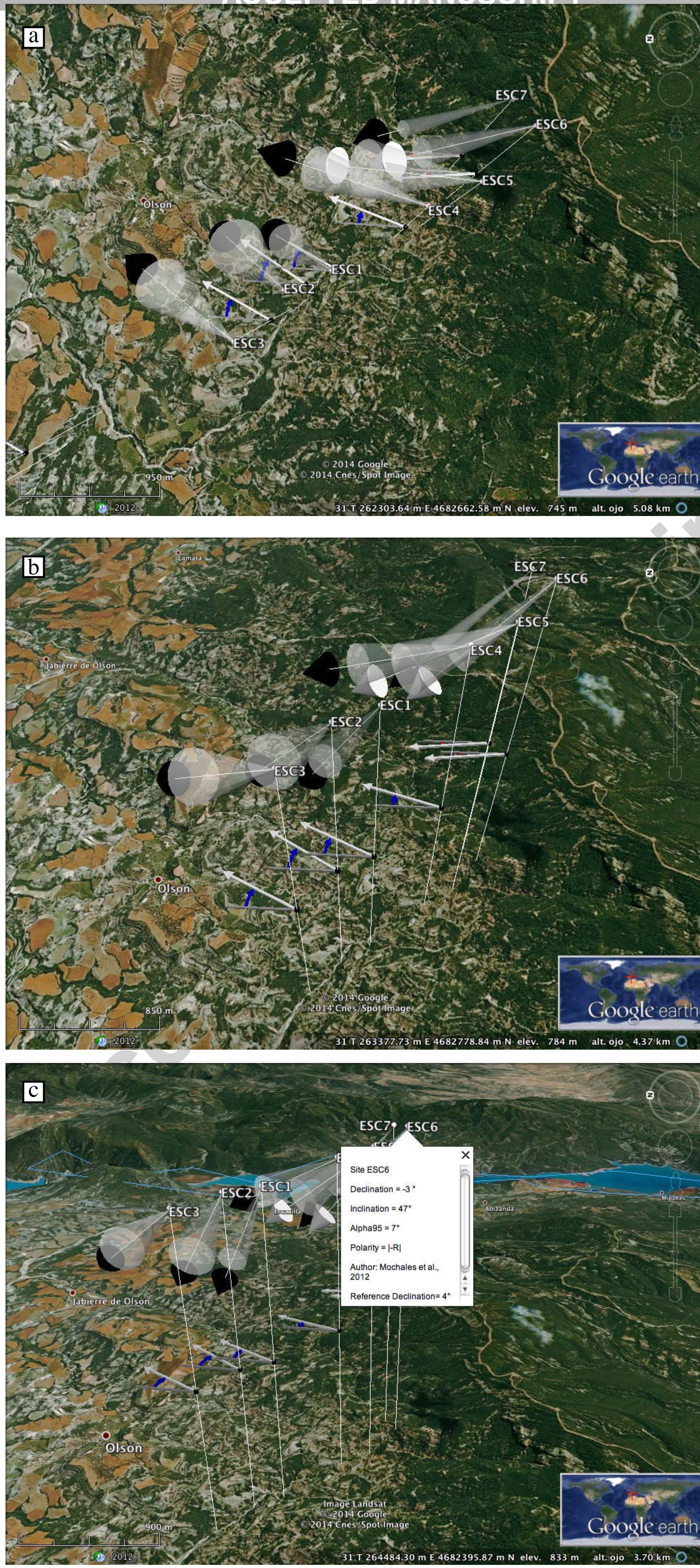
a
ESC7
ESC6
ESC5
ESC4
Olson
ESC1
ESC2
ESC3
© 2014 Google
© 2014 Cnes/Spot Image
950 m
2012
Google earth
31 T 262303.64 m E 4682662.58 m N elev. 745 m alt. ojo 5.08 km
b
Lamata
Jabierre de Olson
ESC7
ESC6
ESC5
ESC4
ESC1
ESC2
ESC3
Olson
© 2014 Google
© 2014 Cnes/Spot Image
850 m
2012
Google earth
31 T 263377.73 m E 4682778.84 m N elev. 784 m alt. ojo 4.37 km
c
ESC7
ESC6
ESC2
ESC1
ESC3
Abizanda
Jabierre de Olson
Olson
Site ESC6
Declination = -3 °
Inclination = 47°
Alpha95 = 7°
Polarity = |-R|
Author: Mochales et al., 2012
Reference Declination= 4°
Image Landsat
© 2014 Google
© 2014 Cnes/Spot Image
900 m
2012
Google earth
31 T 264484.30 m E 4682395.87 m N elev. 833 m alt. ojo 3.70 km

Figure 5

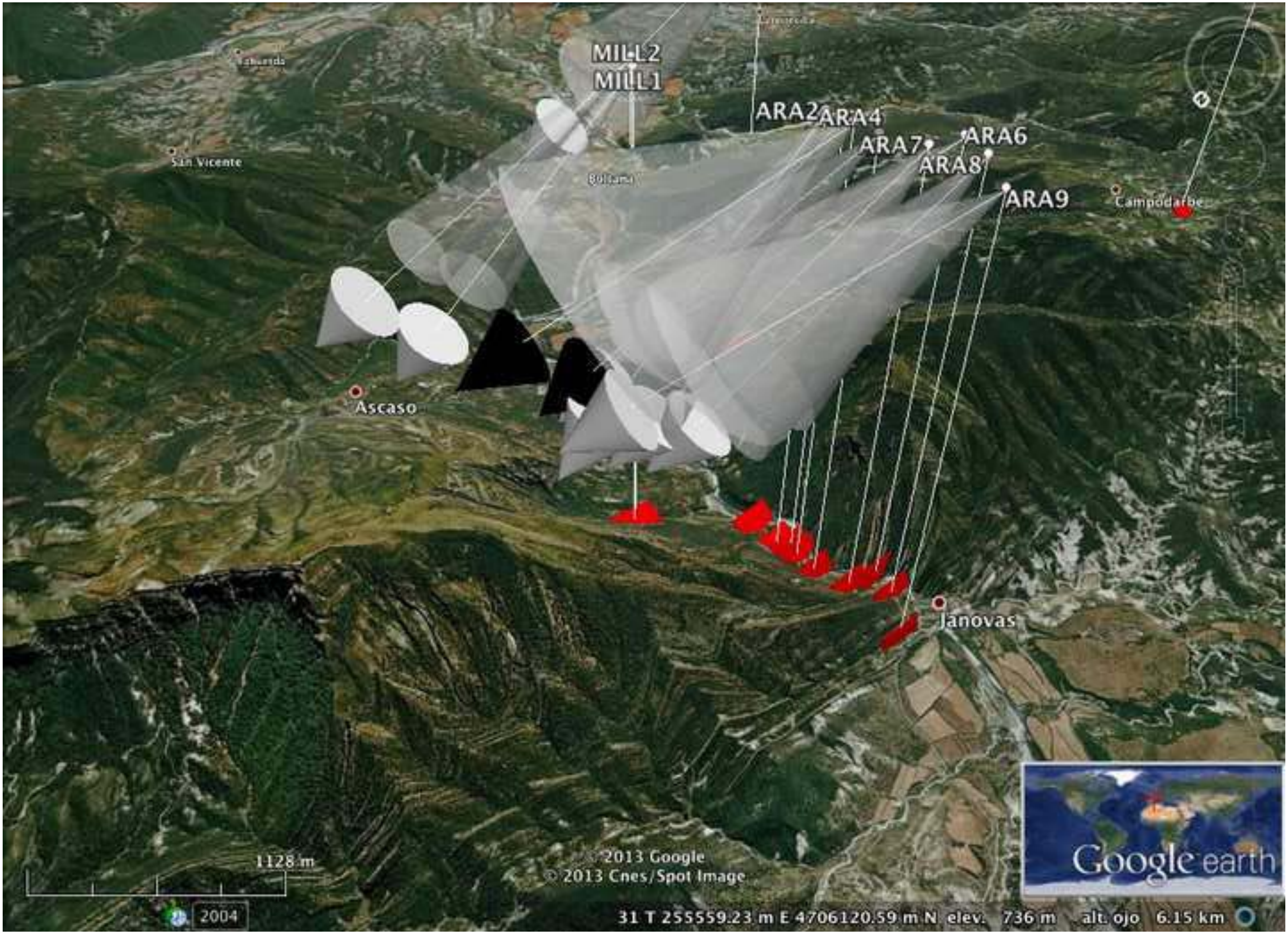
MILL2
MILL1
ARA2
ARA4
ARA7
ARA6
ARA8
ARA9
San Vicente
Campodarbe
Ascaso
Janovas
1128 m
© 2013 Google
© 2013 Cnes/Spot Image
Google earth
2004
31 T 255559.23 m E 4706120.59 m N elev. 736 m alt. ojo 6.15 km

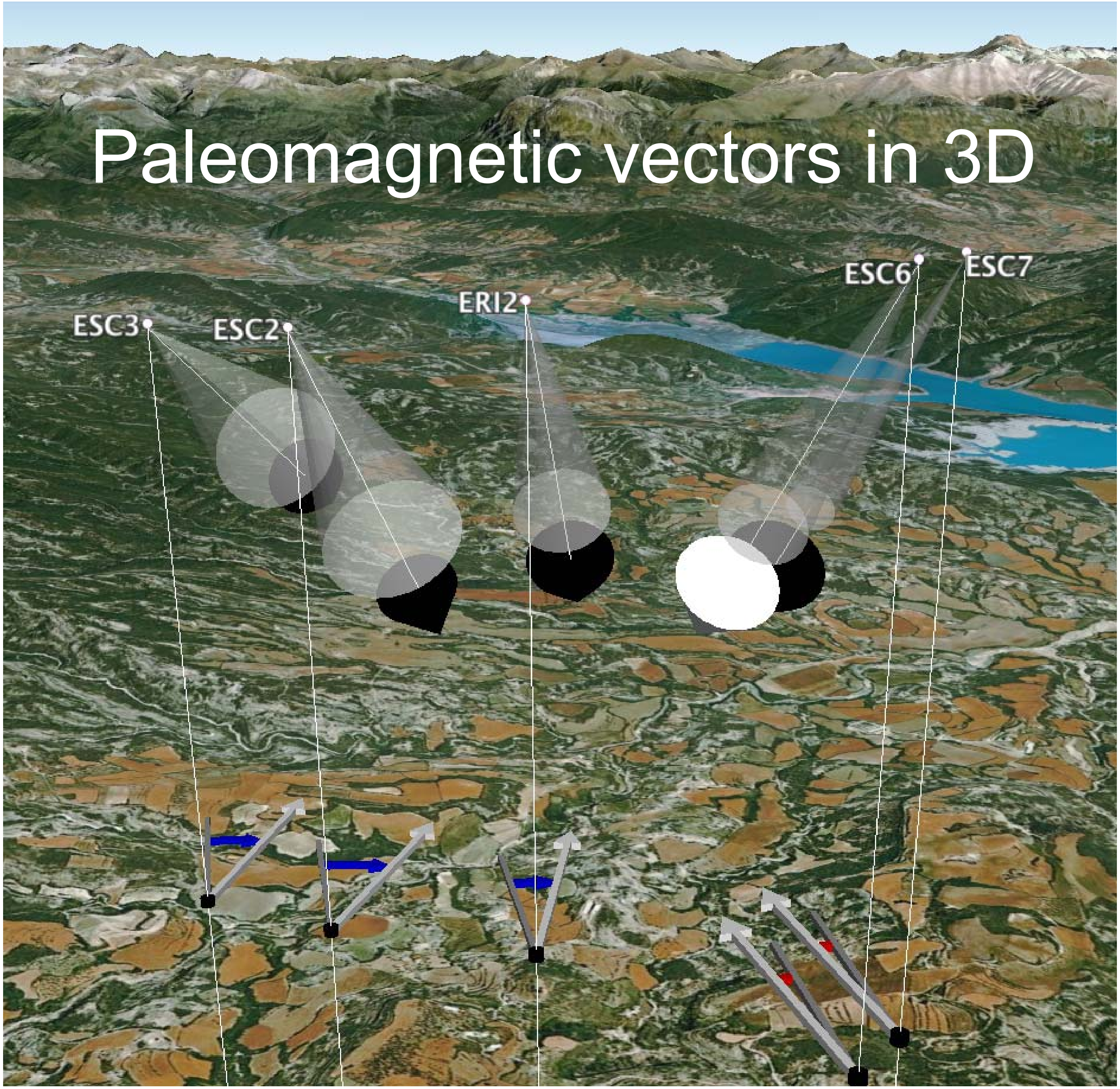
Paleomagnetic vectors in 3D
ESC3
ESC2
ERI2
ESC6
ESC7